
[View Journal Online](#)
[View Article Online](#)

Structural study of three heteroaryl oximes, heteroaryl-N=OH: Compounds forming strong C3 molecular chains

John Nicolson Low ¹, James Lewis Wardell ^{1,2}, Cristiane Franca da Costa ²,
 Marcus Vicinius Nora Souza ² and Ligia Rebelo Gomes ^{3,4,*}

¹ Department of Chemistry, University of Aberdeen, Meston Walk, Old Aberdeen, AB24 3UE, Scotland
 jnlow111@gmail.com (J.N.L.), jms_wardell@yahoo.co.uk (J.L.W.)

² Instituto de Tecnologia em Fármacos e Farmanguinhos, Fundação Oswaldo Cruz, 21041-250 Rio de Janeiro, Rio de Janeiro, Brazil
 crisfrancaufj@gmail.com (C.F.C.), marcos_souza@far.fiocruz.br (M.N.S.)

³ FP-ENAS-Faculdade de Ciências de Saúde, Escola Superior de Saúde da UFP, Universidade Fernando Pessoa, Rua Carlos da Maia, 296, P-4200-150 Porto, Portugal
 lrgomes@ufp.edu.pt (L.R.G.)

⁴ REQUIMTE, Departamento de Química e Bioquímica, Faculdade de Ciências da Universidade do Porto, Rua do Campo Alegre, 687, P-4169-007, Porto, Portugal

* Corresponding author at: FP-ENAS-Faculdade de Ciências de Saúde, Escola Superior de Saúde da UFP, Universidade Fernando Pessoa, Rua Carlos da Maia, 296, P-4200-150 Porto, Portugal.

Tel: +351.22.5074630 Fax: +351.22.5074637 e-mail: lrgomes@ufp.edu.pt (L.R. Gomes).

RESEARCH ARTICLE

ABSTRACT



doi: 10.5155/eurjchem.9.3.151-160.1734

Received: 14 May 2018

Received in revised form: 04 June 2018

Accepted: 05 June 2018

Published online: 30 September 2018

Printed: 30 September 2018

KEYWORDS

Oximes
 Hydrogen bonds
 X-ray crystallography
 Molecular interactions
 Heteroaryl compounds
 Hirshfeld surface calculations

In order to further investigate the structural chemistry of oximes and to further establish the main structural arrangements adopted, we have determined the crystal structure of and carried out Hirshfeld surface calculations on three heteroaryl oximes, namely (*Z*)-thiophene-2-carbaldehyde oxime (1), (*Z*)-1*H*-pyrrole-2-carbaldehyde oxime (2) and (*Z*)-5-nitrofuran-2-carbaldehyde oxime (3). As confirmed by both techniques, the major intermolecular interactions in each compound are classical N—H···O hydrogen bonds, which link the molecules into C3 chains. Such an arrangement has been previously reported as an important aggregation mode for oximes. Secondary interactions, C—H···π and C—H···O interactions, in compounds 1 and 2, and interactions involving the nitro group oxygen atoms in compound 3 link the chains into three dimensional arrays.

Cite this: *Eur. J. Chem.* 2018, 9(3), 151-160

Journal website: www.eurjchem.com

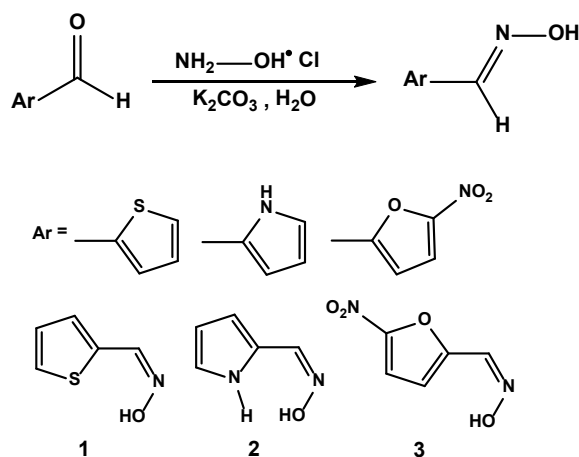
1. Introduction

The oxime group, R₁R₂C=NOH, is found in many biologically active compounds [1,2], with a wide range of uses including as antitumor agents [3-6], acaricidal and insecticidal agents [7], thymidine phosphorylase inhibitors [8], antimicrobial agents [9], bactericides [10], anti-inflammatory agents [11] and in the treatment of nerve-gas poisoning [12-15]. In the plant kingdom, oximes play a vital role in metabolisms [16].

As an important group of organic compounds, it is not surprising that crystal structures of various oximes have attracted attention [16-19]. Oximes with their =N-OH functional group are ideally arranged for classical hydrogen bonding. The last survey of the classical hydrogen bonding patterns in oximes reported in 2010 by Low *et al.* [19] confirmed that the most frequently found arrangements in oximes are R₂(6) dimers and C3 chains, see Figure 1.

Hydrogen bonds are considered as the strongest and most directional of intermolecular interactions available in molecules [20] and thus play the major roles in determining the overall supramolecular structures. However the involvement of weaker intermolecular interactions, such as C—H···O hydrogen bonds and C—H···π interactions can have further significant influences [21].

We have continued our studies of oximes by determining the crystal structures of three five-membered heteroaryl oximes, namely (*Z*)-thiophene-2-carbaldehyde oxime (1), (*Z*)-1*H*-pyrrole-2-carbaldehyde oxime (2) and (*Z*)-5-nitrofuran-2-carbaldehyde oxime (3) Scheme 1. In each case, classical O—H···N hydrogen bonds form the C3 chains. Also present generally in compounds 1-3 are C—H···O and C—H···π interactions. The structural features have been also analysed by computing the Hirshfeld surfaces mapped over d_{norm}.



Scheme 1. Synthetic route and schematic representation of compounds 1-3.

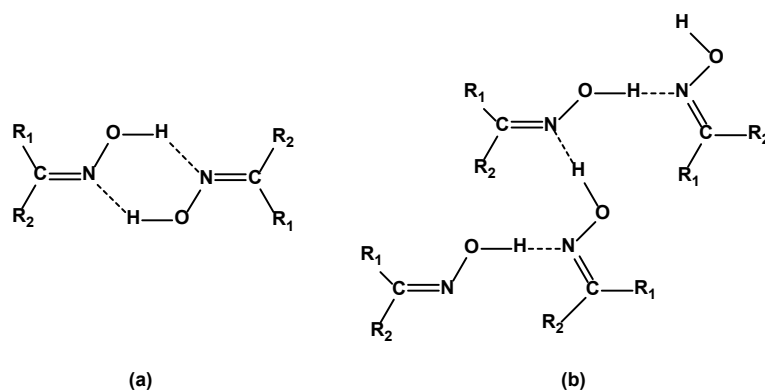


Figure 1. The most common hydrogen bonding motifs in oximes: (a) representative $R_2(6)$ ring (b) representative C3 chain.

2. Experimental

2.1. Synthesis

The compounds, 1-3, were generally prepared on refluxing the corresponding aldehyde with hydroxylamine in an aqueous solution containing potassium carbonate, following a general procedure [22]: a mixture of an aldehyde (2 mmol), hydroxylamine hydrochloride (2.2 mmol) and potassium carbonate (4 mmol) in water (20 mL) was refluxed for 1 hour. The reaction mixture was extracted into ether, dried over magnesium sulphate and rotary evaporated. The solid residue was recrystallised twice from ethanol. (Scheme 1). The samples used in the structure determinations were further recrystallized from methanol. Compound 1: M.p.: 131-143 °C: Lit. [23] M.p.: 132-136 °C; Compound 2: M.p.: 161-163 °C: Lit. [24] M.p.: 163-166 °C; Compound 3: M.p.: 121-122 °C: Lit. [25] M.p.: 121-122 °C.

2.2. Experimental crystallography

Data collection, data reduction and cell refinement utilized CrysAlis PRO 1.171.39.9g [26] for compounds 1 and 3, and CrysAlis PRO 1.171.39.30d [27] for compound 2. For all compounds, programs used to solve structures were OSCAIL [28], SHELXT [29] and programs used to refine structure were OSCAIL [28], ShelXle [30] and SHELXL2017/1 [31]. The molecular graphics program was Mercury [32] and PLATON [33]. Software used to prepare material for publication were OSCAIL [28] SHELXL2017/1 [31], Absorption corrections were

carried out using Multi-scan *CrysAlis PRO* 1.171.39.9g [26] with empirical absorption correction using spherical harmonics, implemented in SCALE3 ABSPACK scaling algorithm. The positions of the hydroxyl hydrogens were located in the difference map, and refined as riding atoms and rotating group about the N-O bonds. Other H atoms were treated as riding atoms with C-H (aryl) and C-H(alkyl) = 0.95 and 0.99 Å.

2.3. Hirshfeld surfaces analysis

The Hirshfeld surfaces and two-dimensional fingerprint (FP) plots [34] were generated using Crystal Explorer 3.1 [35]. The Hirshfeld surface mapped over d_{norm} is scaled between -0.750 to 1.560.

3. Results and discussion

Crystal data and structure refinement details are listed in Table 1. As the bond angles and lengths fall in the normal regions found for these compounds, they are not further discussed here. There are two similar but independent molecules in both the asymmetric units of compounds 1 and 2, (**Mol A** and **Mol B** in both cases), while only one molecule is found in the asymmetric unit of compound 3. All three compounds crystallize in *orthorhombic* phases: compound 1 in the $Pca2_1$ space group, with $Z = 8$, compound 3 in the space group $P2_12_12_1$ with $Z = 8$ and compound 2 in the $Pna2_1$ space group with $Z = 4$.

Table 1. Crystal data and details of the structure refinement for compound 1-3.

Parameters	Compound 1	Compound 2	Compound 3
Empirical formula	C ₅ H ₅ NOS	C ₅ H ₅ N ₂ O	C ₅ H ₄ N ₂ O ₄
Formula weight	127.16	110.12	156.10
Temperature (K)	100	100	100
Crystal system	Orthorhombic	Orthorhombic	Orthorhombic
Space group	<i>Pca</i> 2 ₁	<i>Pna</i> 2 ₁	<i>P2</i> ₁ 2 ₁ 2 ₁
a, (Å)	11.4684(3)	6.9338(1)	5.2711(2)
b, (Å)	13.6834(5)	11.2109(1)	5.5198(2)
c, (Å)	7.3641(2)	13.7319(1)	21.2019(7)
Volume (Å ³)	1155.62(6)	1067.44(2)	616.88(4)
Z	8	8	4
ρ _{calc} (g/cm ³)	1.462	1.370	1.681
μ (mm ⁻¹)	0.45	0.83	0.15
F(000)	528	464	320
Crystal size (mm)	0.20 × 0.03 × 0.02	0.20 × 0.15 × 0.05	0.08 × 0.07 × 0.03
Radiation	MoKα (λ = 0.71073)	MoKα (λ = 0.71073)	MoKα (λ = 0.71073)
θ range for data collection (°)	1.488 to 27.482	5.093 to 68.199	1.921 to 27.478
Index range	-14 ≤ h ≤ 12 -12 ≤ k ≤ 17 -8 ≤ l ≤ 9	-8 ≤ h ≤ 8 -13 ≤ k ≤ 13 -16 ≤ l ≤ 16	-6 ≤ h ≤ 6 -7 ≤ k ≤ 7 -27 ≤ l ≤ 27
Reflections collected	8080	18404	8390
Independent reflections	2459	1945	1411
Observed reflections [I ≥ 2σ(I)]	2518 [R _{int} = 0.021]	2518 [R _{int} = 0.029]	2518 [R _{int} = 0.019]
Data/restraint/ parameters	2518/154/1	1945/161/1	1411/104/0
Goodness-of-fit on F ²	1.09	1.06	1.07
Final R indexes [I ≥ 2σ(I)]	R ₁ = 0.035; wR ₂ = 0.099	R ₁ = 0.024; wR ₂ = 0.063	R ₁ = 0.021; wR ₂ = 0.056
Final R indexes [all data]	R ₁ = 0.035; wR ₂ = 0.099	R ₁ = 0.024; wR ₂ = 0.063	R ₁ = 0.024; wR ₂ = 0.063
Largest diff. peak/hole (e.Å ⁻³)	0.49	0.13	0.19
Absolute structure	Refined as an inversion twin	Refined as a perfect inversion twin	Refined as a perfect inversion twin
Flack parameter	0.39(12)	0.5	0.5
CCDC number	1839089	1839091	1839090

Molecules of the thienyl derivative, **1**, exhibit small percentages (5 %) of disorder (flip disorder) involving a 180 ° rotation about C12—C121 bond in Mol A and C22—C221 in Mol B. Such disorder is a fairly common finding for thienyl derivatives [36]. The atom arrangements and numbering schemes for all molecules, excluding the minor component of compound **1**, are illustrated in Figure 2. Due to the very small extent of the disorder and the lack of any directional involvement of the sulfur atom in the intermolecular interactions, the minor component has been ignored in the structural discussion.

As shown in Figure 2, there are different arrangements of the CH=NOH side chains, w.r.t the heteroaryl group, in compound **3**, on one hand, and in compounds **1** and **2**, on the other. The set-up in compound **2** allows the formation of classical intramolecular N—H...O hydrogen bonds. The intramolecular S...O separations in the two independent molecules of compound **1** are 2.691(3) and 2.703(2) Å, which are well within the sum of the contact radii of 3.32 Å, and do suggest a positive interaction. Intramolecular S...O interactions have been well reported [37,38]. The molecular conformation of compound **3** precludes any O—H...O classical intramolecular hydrogen bonds but instead allows a weak C—H...O interaction.

3.1. Intermolecular interactions

A complete list of the intermolecular interactions is shown in Table 2. As well as the strong classical O—H...N hydrogen bonds, each compound exhibits weaker C—H...O hydrogen bonds and C—H...π interactions. In compound **3**, there are additional interactions involving the two oxygen atoms of its nitro substituent. The only heteroatoms in the aryl units to be involved in interactions are those in compound **2**.

As indicated in the article by Low et al. [19], oximes commonly use the strong classical O—H...N intermolecular hydrogen bonds to form R₂²(6) dimers or C3 chains, see Figure 1. Each of the three compounds studied here use such bonds to form the C3 chains, as illustrated in Figures 3a, 4a and 5a, for compounds **1**, **2** and **3**, respectively. These hydrogen-bonding

chains form the backbone of the structures. However the additional weaker intermolecular interactions are involved in augmenting the strength of the chain and linking the C3 chains into more elaborate arrangements.

In the case of compound **1**, the augmentation of the chains is provided by C121—H121...O123 hydrogen bonds and C13—H13...π interactions, see Figure 3b. With involvement of the weaker C121—H121...O123 hydrogen bonds, R₃³(8) rings are present within the C3 chains. The C3 chains are linked by C221—H221...π interactions into a three dimensional array: Figure 3c illustrates the linkage of two partial C3 chains drawn in different colors.

In the case of compound **2**, the augmentation of the chains is provided by three different interactions within a C3 chain: C221—H221...O223 hydrogen bonds and C15—H15...π (Mol A) and C23—H23...π (Mol B) interactions, see Figure 4b. Similar to the situation in compound **1**, R₃³(8) rings are derived within the C3 chains from the involvement of the weaker C221—H221...O223 hydrogen bonds. In the case of compound **2**, more complex linkages of the C3 chains into a three-dimensional array occur from the involvement of various other weaker intermolecular interactions. Despite the differences in the intermolecular interaction in compounds **1** and **2**, the two compounds possess similar packing arrangements, see Figure 6.

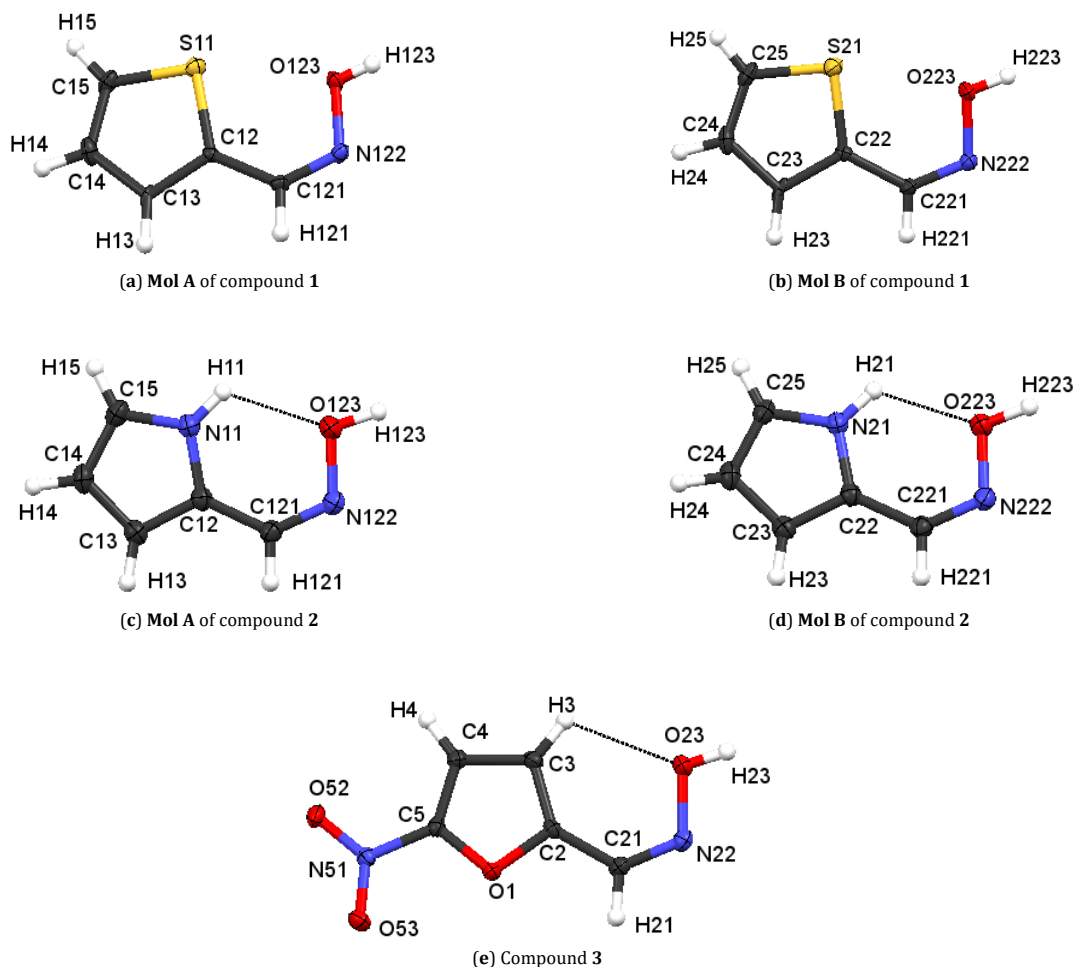
The situation in compound **3** is somewhat different from those in compounds **1** and **2**. Unlike the situation in compounds **1** and **2**, there are no additional interactions within a C3 chain and links between the C3 chains are solely generated from interactions involving the nitro group oxygen atoms, namely C3—H3...O53 and C4—H4...O52 hydrogen bonds and N52—H52...π interactions. In each of these three interactions, forms different connections: Figures 5b-d illustrate some interchain interactions. Figure 6c contrasts the packing of compound **3** with those of compounds **1** and **2**.

3.2. Hirshfeld surfaces analysis

The Hirshfeld surfaces and two-dimensional fingerprint (FP) plots [34,35] provide complementary information concerning the intermolecular interactions discussed upper.

Table 2. Geometric parameters and symmetry operations for hydrogen bonds and intermolecular interactions (Å, °).

Compound	D—H...A	D—H	H...A	D...A	D—H...A	Symmetry code	
Intramolecular hydrogen bonds							
2	N11—H11...O123	0.89(2)	2.14(3)	2.657(2)	116.7(18)	-	
2	N21—H21...O223	0.91(2)	2.09(3)	2.658(2)	119.2(19)	-	
3	C3—H3...O23	0.95	2.40	2.8039(16)	105	-	
Intermolecular hydrogen bonds							
1	O123—H123...N222	0.78(5)	1.96(5)	2.743(4)(17)	177(6)	x, y, z	
1	O223—H223...N122	0.85(5)	1.90(6)	2.749(4)	178(8)	$1/2-x, y, -1/2+z$	
1	C121—H121...O123	0.95	2.52	3.316(4)	142	$1/2-x, y, 1/2+z$	
2	O123—H123...N222	0.94(3)	1.80(3)	2.728(2)	170(3)	$-1/2+x, 1/2-y, z$	
2	O223—H223...N122	0.97(3)	1.78(3)	2.754(2)	177(2)	x, y, z	
2	C221—H221...O223	0.95	2.60	3.372(2)	139	$1/2+x, 1/2-y, z$	
3	O23—H23...N22	0.87(2)	1.93(2)	2.7876(15)	170.3(19)	$1/2+x, 5/2-y, 1-z$	
3	C3—H3...O53	0.95	2.48	3.3604(15)	155	$1+x, 1+y, z$	
3	C4—H4...O52	0.95	2.38	3.2043(16)	144	$2-x, 1/2+y, 3/2-z$	
Y—X...π interactions							
Compound	Y—X...Cg ^a	X...Cg	X _{perp} ^b	γ ^c	Y—X...Cg	Y...Cg ^d	Symmetry code
1	C13—H13...Cg1 (Mol A) ^e	2.96	2.93	7.49	157	3.854(3)	$1/2-x, y, 1/2+z$
1	C221—H221...Cg2 (Mol B) ^e	2.54	2.54	1.36	168	3.476(4)	$1-x, 1-y, 1/2+z$
2	C15—H15...Cg1 (Mol A) ^e	2.72	2.70	7.42	138	3.488(2)	$-1/2+x, 1/2-y, z$
2	N21—H21...Cg1 (Mol A) ^e	2.73(3)	2.69	9.14	146(2)	3.5199(17)	$1-x, 1-y, -1/2+z$
2	C23—H23...Cg2 (Mol B) ^e	2.79	2.78	4.58	148	3.637(2)	$1/2+x, 1/2-y, z$
2	C121—H121...Cg2 (Mol B) ^e	2.48	2.48	1.90	163	3.406(2)	$2-x, 1-y, 1/2+z$
3	N51—O52...Cg1 ^e	3.4950(11)	3.152	25.59	91.63(7)	3.7379(12)	$x, -1+y, z$

^a Center of gravity of ring J (Plane number above).^b Perpendicular distance of H to ring plane J.^c Angle between Cg-H vector and ring J normal.^d Distance between C-atom and the nearest carbon atom in the aromatic ring.^e Cg1 and Cg2 for compound 1 are the centroids of the ring containing S11 and S21, respectively. Cg1 and Cg2 for compound 2 are the centroids of the ring containing N11 and N21, respectively. Cg1 for compound 3 is the centroid of the ring containing O1.**Figure 2.** Atom arrangements and numbering schemes for compounds 1-3. Probability ellipsoids have been drawn at the 50% level. Intermolecular hydrogen bonds have been drawn as dashed lines.

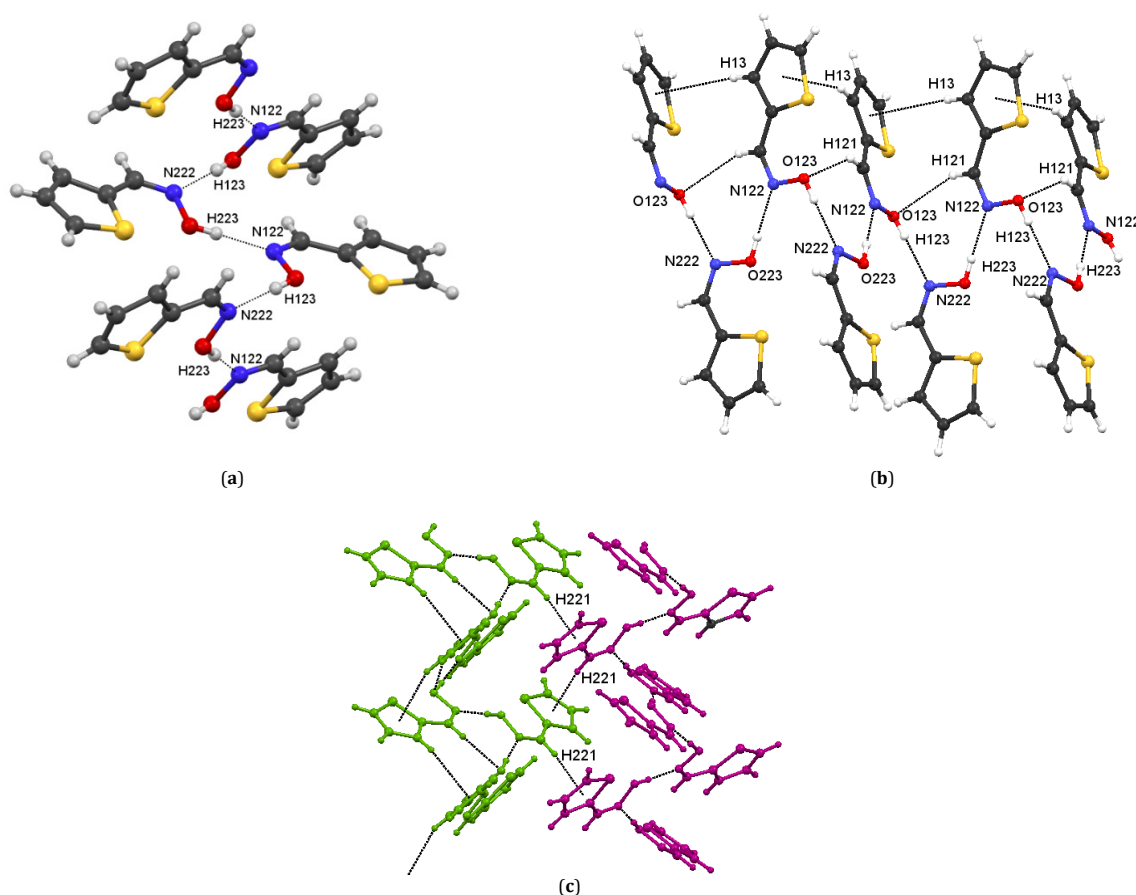


Figure 3. Compound 1, (a) A part of a C3 chain, generated from alternating **Mol A** and **Mol B** units, linked by classical O123—H123...N222 and O223—H223...N122 hydrogen bonds, (b) part of the arrangement generated from the involvement of additional C13—H13... π interactions and C121—H121...O123 hydrogen bonds within a C3 chain, drawn in different colors, by C221—H221... π interactions. Intermolecular interactions are drawn as thin dashed lines. Symmetry operations are listed in Table 2.

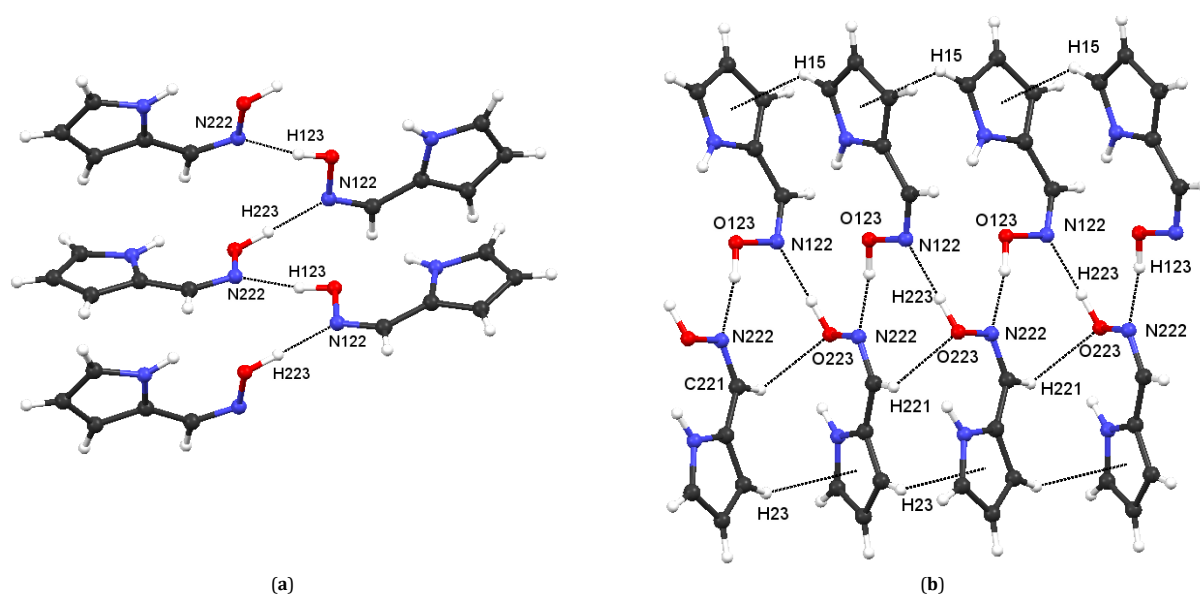


Figure 4. Compound 2, (a) A part of a C3 chain, generated from alternating **Mol A** and **Mol B** units, linked by classical O123—H123...N222 and O223—H223...N122 hydrogen bonds, (b) part of the arrangement generated from the involvement of additional C15—H15... π (**Mol A**) and C23—H23... π (**Mol B**) interactions and C121—H121...O123 hydrogen bonds within a C3 chain. Intermolecular interactions are drawn as thin dashed lines. Symmetry operations are listed in Table 2.

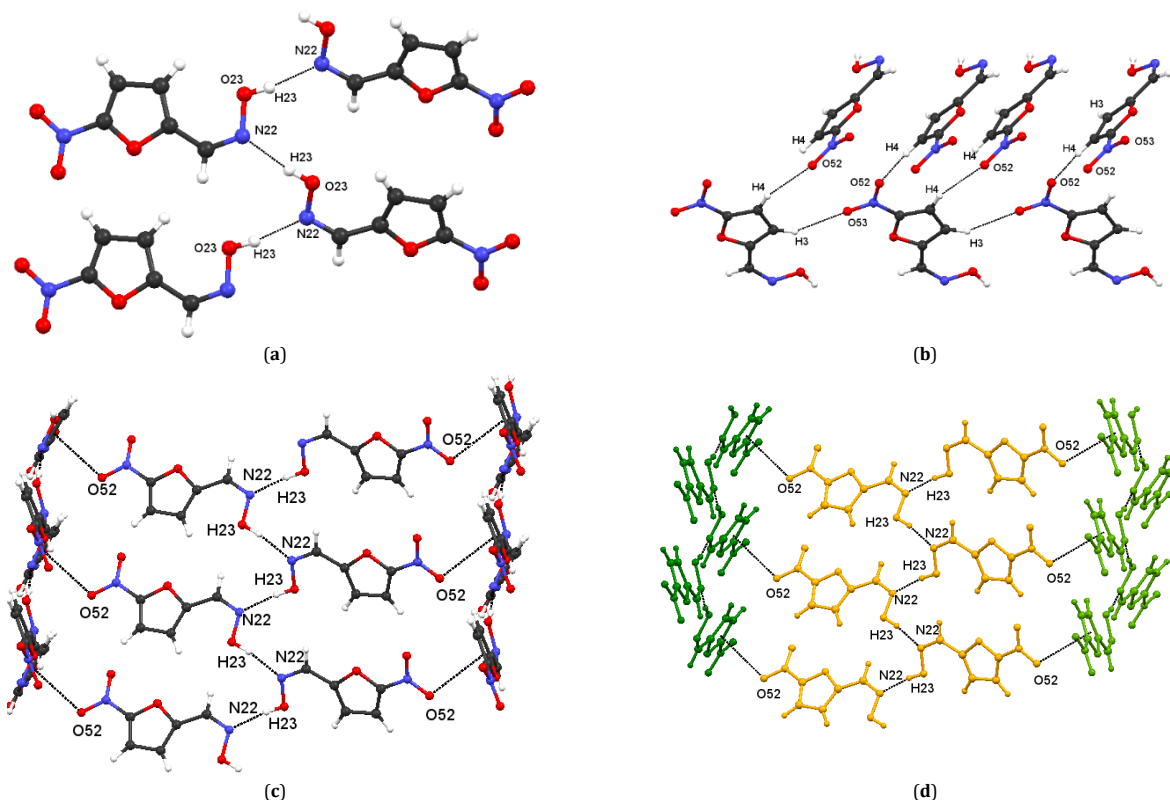


Figure 5. Compound 3, (a) A part of a C3 chain of molecules generated from classical O23—H23...N22 hydrogen bonds, (b) an illustration of the linkage of molecules from different C3 chains by C4—H4...O52 and C3—H3...O53 hydrogen bonds, (c) an illustration of the linkage of C3 chains by N22—H23... π interactions, (d) a view of Figure 5b using different colours for the C3 chains. Intermolecular interactions are drawn as thin dashed lines. Symmetry operations are listed in Table 2.

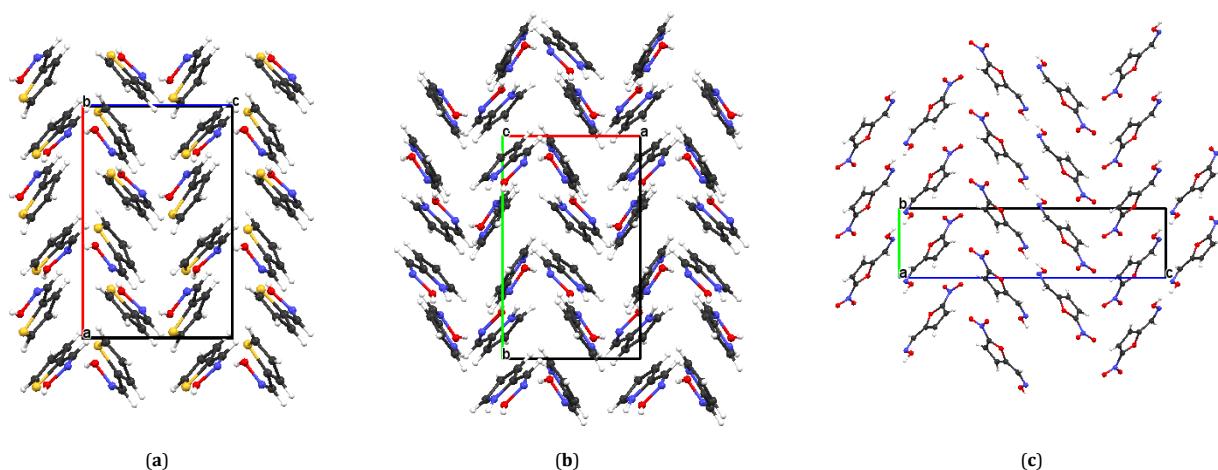


Figure 6. Packing arrangements of compounds 1 (a), 2 (b) and 3 (c).

The structural features of compounds 1-3 will be analysed by computing the Hirshfeld surfaces mapped over d_{norm} (-0.680 to 1.16 range). As said, compound 1 presents two molecules in the asymmetric unit that are identified as **Mol A** and **Mol B**. The Hirshfeld surface of **Mol A** is depicted in Figure 7 in two views.

The left frame shows two pair sets of red spots, one pair with a spreader area that is due to the contacts involving the nitrogen and the oxygen atoms of the oxime, those making a C(3) chain. The other pair of spots are due to O...H-C close contacts involving the acidic hydrogen atom H121 and the O123 oxygen atom. The right hand frame shows a pair of light

red spots that are close S...C close contacts. **Mol B** presents the corresponding N...H-O contacts with **Mol A**, those give the two strong red spots that are complementary to the spots near the atoms involved in the same interactions in **Mol A**. **Mol B** also presents S...C close contacts as detected by red spot areas shown in the right frame of Figure 8 and contacts involving the acidic H atom H221 but, in contrast with **Mol A**, the hydrogen atom establishes contacts with all atoms of the thiophene ring giving spots looking like "flower petals" in the Hirshfeld surface (left frame, Figure 8, those include the C-H... π interactions).

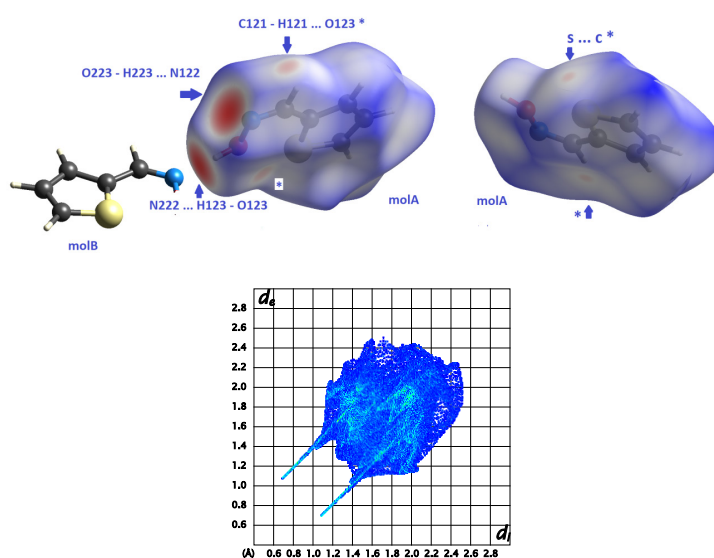


Figure 7. Views of both faces of the Hirshfeld surface mapped over d_{norm} for compound **1 (Mol A)**. The highlighted red spots on the left picture indicate contact points with the atoms participating in the O—H...N and C—H...O intermolecular interactions. The picture in the right side show the other face of the surface; the bright red areas that suggest for the existence of S...C contacts. The N...H close contacts are responsible for the pair of sharp spikes in the FP plot that end at d_e/d_i near 1.1 Å.

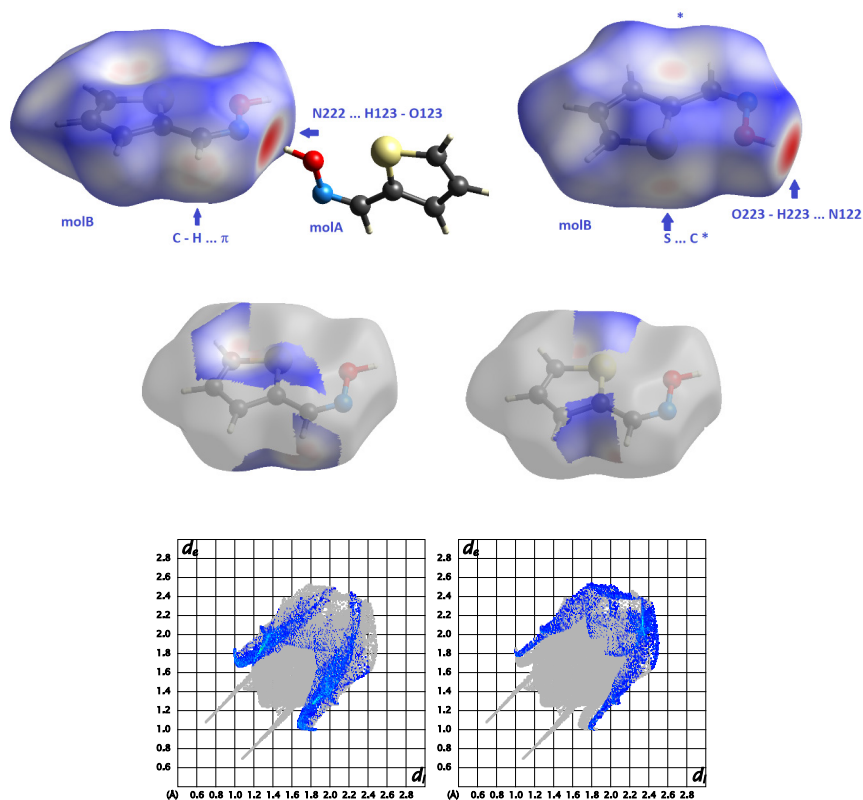


Figure 8. Views of the Hirshfeld surface mapped over d_{norm} (up) and fingerprint plot (down) for compound **1 (Mol B)**. The large red areas in the HS correspond to the O—H...N contacts; The looking like “flower petals” in the Hirshfeld surface of the left picture are due to close contacts between the acidic H atom and the carbon and sulphur atoms of the thiophene ring. Those contacts are confirmed by the analysis of the FP plots for the molecule (see the bottom figure of the HS for details). FP plot in the left shows a pair of wings that are due to close H ... C contacts while the FP plot on the right side shows wings that are due to H...S close contacts).

Those short contacts are perfectly identified in the FP plot of the **Mol B**, that is depicted in **Figure 8**, down, together with the HS. In **Table 3**, the percentages of atom...atom close

contacts are given. Apart from the H...H contacts, relevant contacts are of C...H/H...C and S...H/H...S type in both molecules, followed by the N...H/ H...N and O...H/ H...O ones.

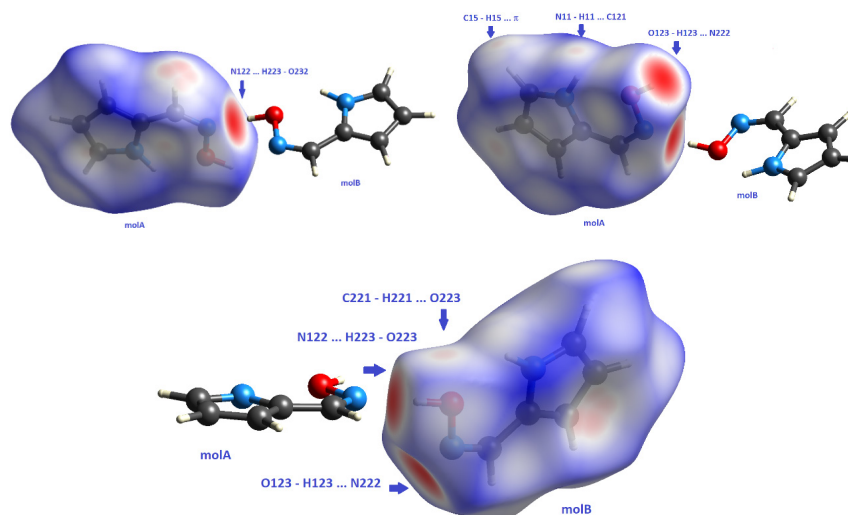


Figure 9. Views of the Hirshfeld surface mapped over d_{norm} for compounds **2** (**Mol A**) (up) and (**Mol B**) (down). The large red areas in the HS correspond to the O—H...N contacts; The looking like “flower petals” in the Hirshfeld surface are due to close contacts between the H121 atom and the nitrogen and carbon atoms of the pyrrolic ring. As in compound **1**, those contacts were confirmed by the analysis of the FP plots for the molecule.

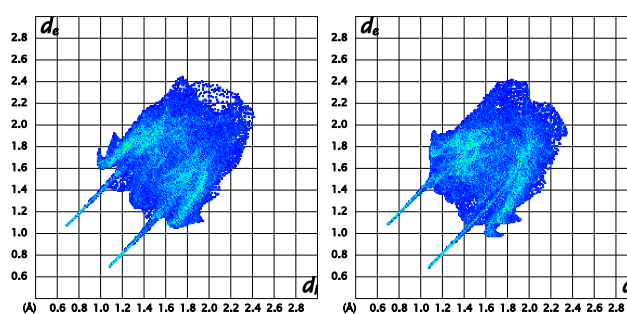


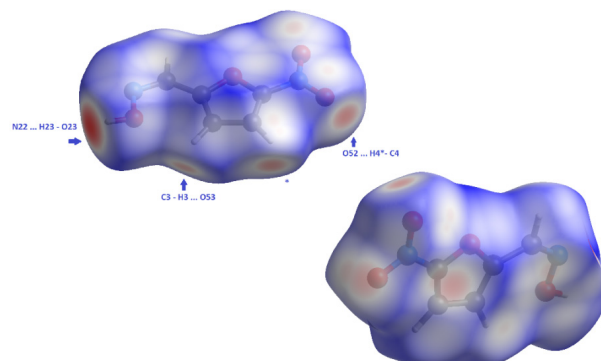
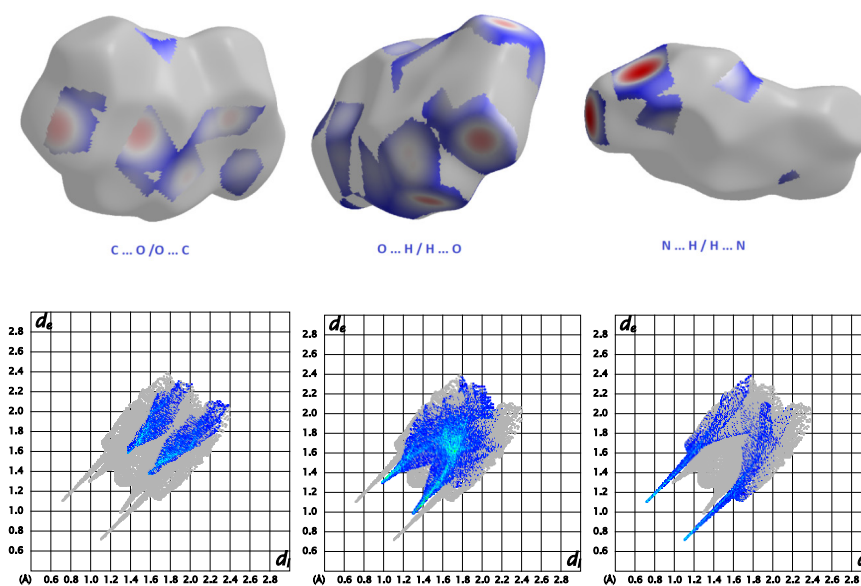
Figure 10. The FP plots for compound **2** (**Mol A**) (right) and **Mol B** (left) show a couple of spikes corresponding to N...H contacts. The asymmetric shape of the wings in the FP plots, left side in FP plot of **Mol A** and right side in **Mol B** include to the N...H and C...H contacts with the pyrrole involving the H atom H15.

Compound **2** presents two molecules (**Mol A** and **Mol B**) in the asymmetric unit as well. The HS reveal several red areas as can be viewed in [Figure 9](#). The upper pictures show the HS for **Mol A**, where a pair of spread red areas parallel to the OH group and to the nitrogen atom of the oxime can be visualised, those are surfaces that show close contacts involving the oxime: those are the N...H/H...N contacts that make chains in a similar way as described for compound **1** connecting **Mol A** with **Mol B**. Apart from those red areas, a set of red regions that presents complementary intensity and shape has been also detected by the HS calculations, one near the hydrogen atom H15 of **Mol A** (see frame right and above) and another parallel to the heterocycle ring of the same molecule suggesting for the existence of close contacts involving the referred H atom and the ring. Finally there is a set of light red spots in the HS of **Mol A** near H atom H121 that has correspondence in intensity and shape in **Mol B** that account for H... π contacts. The FP plots ([Figure 10](#)) for **Mol A** and **Mol B** display a couple of spikes corresponding to N...H contacts. The asymmetric shape of the wings in the FP plots, left side in FP plot of **Mol A** and right side in **Mol B** include to the N...H and C...H contacts with the pyrrole involving the H atom H15. The contributions from various atom to atom contacts for both molecules of compound **2**, are listed in [Table 3](#). Apart from the H...H contacts the most significant are the H...O/O...H that are higher than 25%.

The presence of the nitro substituent in compound **3** increases the possibility of the establishment of close O...H contacts. This is confirmed by the HS analysis for the compound but, in spite of that, the prevalent contacts are of C...H type, as can be confirmed by the % of atom to atom close contacts in [Table 3](#). Several views of the HS surface are depicted in [Figure 11](#). Apart from the N...H/H...N close contact due to the N22...H23-O23 hydrogen bond (identified in [Figure 4](#)), the surface presents a set of red areas near the oxygen atoms of the nitro group that are complementary in shape and size with those being near the hydrogen atoms of the pyran ring suggesting for O...H interactions, as can be visualised in [Figure 11](#). In addition the surface shows several other red areas also near the nitro oxygen atoms and in the area parallel to the aromatic ring that are probably due to O...C close contacts. The nature of those contacts is confirmed by the partial analysis of the HS surface based on the element contacts given by the PF plot of the surface, as can be visualized in the frames of [Figure 12](#). The FP for **3** displays two pairs of spikes; the outer ones ending at $(d_e, d_i) \cong (1.1, 0.7)$ Å (and *vice versa*) corresponding to the N...H/H...N contacts and the inner ones ending at $(d_e, d_i) \cong (1.3, 1.0)$ Å corresponding to the H...O/O...H contacts. The C...O/O...C contacts contribute to high the percentage of atom...atom close contacts involving both elements as can be confirmed in [Table 3](#).

Table 3. Percentages of atom-atom contacts for compound 1-3 (%).

Compound	H...H	H...O/O...H	H...C/C...H	O...C/C...O	H...N/N...H	H...S/S...H	C...S/S...C
1 Mol A	33.0	7.9	18.9	2.8	16.4	11.4	7.9
1 Mol B	30.1	12.0	22.4	0.6	11.7	11.9	6.8
2 Mol A	42.5	5.2	28.5	0.9	21.2	-	-
2 Mol B	42.2	11.0	26.5	0.7	19.3	-	-
3	12.3	39.3	7.2	15.3	12.0	-	-

**Figure 11.** Views of both faces of the Hirshfeld surface mapped over d_{norm} for compound 3 (Mol A). The highlighted red spots on the left picture indicate contact points with the atoms participating in the O—H...N and C—H...O intermolecular interactions. The picture in the right side show the other face of the surface; the bright red areas that suggest for the existence of S ... C contacts. The N...H close contacts are responsible for the pair of sharp spikes in the FP plot that end at d_e/d_i near 1.1 Å.**Figure 12.** Views of the Hirshfeld surface mapped over d_{norm} (up) and fingerprint plot (down) for compound 3. The highlighted red spots on the the face of the surfaces indicate contact points with the atoms participating in the C...O, H...O and N...H contacts. The FP displays two pairs of spikes; the outer ones ending at $(d_e, d_i) \cong (1.1, 0.7)$ Å (and *vice versa*) corresponding to the N...H/H...N contacts and the inner ones ending at $(d_e, d_i) \cong (1.3, 1.0)$ Å corresponding to the H...O/O...H contacts. The C...O/O...C contacts contribute to high the percentage of atom...atom close contacts involving both elements as can be confirmed in Table 3.

4. Conclusion

The studies confirm that a significant aggregation mode of oximes involves classical N—H...O hydrogen bonds, which provided C3 molecular chains. Further association of the C3 chains into 3-dimensional structures occurs in the case of compounds 1 and 2 from combinations of weaker C—H...O and C-H... π interactions and in the case of compound 3, by interactions involving the nitro group oxygen atoms. The majority of oximes form R^2_2 (6) dimers as opposed to C3 chains which were classically claimed as the usual oxime H-bond pattern [19]. These C3 chains are, in fact, rarely

observed being mostly found in aldoxime structures [19] as is the case here.

Acknowledgements

The authors thank the National Crystallographic Service, University of Southampton, UK, for the data collection, and for their help and advice. LRG thanks the Portuguese Foundation for Science and Technology (FCT) UID/Multi/04546/2013 for support. J.L.W. thanks CNPq, Brazil for support.

Supporting information

CCDC-1839089, CCDC-1839090 and CCDC-1839091 contain the supplementary crystallographic data for compounds **1**, **3**, and **2**, respectively. These data can be obtained free of charge via <https://www.ccdc.cam.ac.uk/structures/>, or by e-mailing data_request@ccdc.cam.ac.uk, or by contacting The Cambridge Crystallographic Data Centre, 12 Union Road, Cambridge CB2 1EZ, UK; fax: +44(0)1223-336033.

Disclosure statement

Conflict of interests: The authors declare that they have no conflict of interest.

Author contributions: All authors contributed equally to this work.

Ethical approval: All ethical guidelines have been adhered.

Sample availability: Samples of the compounds are available from the author.

ORCID

John Nicolson Low

 <http://orcid.org/0000-0003-4743-7448>

James Lewis Wardell

 <http://orcid.org/0000-0003-2195-8827>

Cristiane Franca da Costa

 <http://orcid.org/0000-0001-7385-9201>

Marcus Vicinius Nora Souza

 <http://orcid.org/0000-0003-1566-8110>

Lígia Rebelo Gomes

 <http://orcid.org/0000-0002-3496-6052>

References

- [1]. Abele, E.; Abele, R.; Lukevics, E. *Chem. Heterocycl. Cmpds.* **2018**, *44*, 769-792.
- [2]. Nikitjuka, A.; Jirgensons, A. *Chem. Heterocycl. Cmpds.* **2014**, *49*, 1544-1559.
- [3]. Martinez-Pascual, R.; Meza-Reyes, S.; Vega-Baez, J. L.; Merino-Montiel, P.; Padron, J. M.; Mendoza, A.; Montiel-Smith, S. *Steroids* **2017**, *122*, 24-33.
- [4]. Qin, H. L.; Leng, J.; Youssif, B. G. M.; Amjad, M. W.; Raja, M. A. G.; Hussain, M. A.; Hussain, Z.; Kazmi, S. N.; Bukhari, S. N. A. *Chem. Bio. Drug Des.* **2017**, *90*, 443-449.
- [5]. Canario, C.; Silvestre, S.; Falcao, A.; Alves, G. *Curr. Med. Chem.* **2018**, *25*, 660-686.
- [6]. Huang, G.; Zhao, H. R.; Meng, Q. Q.; Zhang, Q. J.; Dong, J. Y.; Zhu, B. Q.; Li, S. S. *Eur. J. Med. Chem.* **2018**, *143*, 166-181.
- [7]. Dai, H.; Chen, J.; Li, G.; Ge, S. S.; Shi, Y. J.; Fang, Y.; Ling, Y. *Bioorg. Med. Chem. Letters* **2017**, *27*, 950-953.
- [8]. Zhao, S. Y.; Li, K.; Jin, Y.; Lin, J. *Eur. J. Med. Chem.* **2018**, *144*, 41-51.
- [9]. Yadav, P.; Lal, K.; Rani, P.; Mor, S.; Kumar, A.; Kumar, A. *Med. Chem. Res.* **2017**, *26*, 1469-1480.
- [10]. Kozłowska, J.; Potaniec, B.; Zarowska, B.; Aniol, M. *Molecules* **2017**, *22*. Article Number: UNSP 1485
- [11]. Mohassab, A. M.; Hassan, H. A.; Abdelhamid, D.; Abdel-Aziz, M.; Dalby, K. N.; Kaoud, T. S. *Bioorg. Chem.* **2017**, *75*, 242-259.
- [12]. Lorke, D. E.; Kalasz, H.; Petroianu, G. A.; Tekes, K. *Curr. Med. Chem.* **2008**, *15*, 743-753.
- [13]. Voicu, V. A.; Bajgar, J.; Medvedovici, A.; Radulescu, F. S.; Miron, D. S.; S. J. *Appl. Tox.* **2010**, 719-729.
- [14]. Katalinic, M.; Zandona, A.; Ramic, A.; Zorbaz, T.; Primozic, I.; Kovarik, Z. *Molecules* **2017**, *22*, Article number 1234.
- [15]. Radic, Z.; Dale, T.; Kovarik, Z.; Berend, S.; Garcia, E.; Zhang, L.; Amitais, G.; Green, C.; Radi, B.; Duggan, B. M.; Ajami, D.; Rebek, J.; Taylor, P. *Biochem. J.* **2013**, *450*, 231-242.
- [16]. Sorensen, M.; Neilson, E. H. J.; Moller, B. L. *Mol. Plant* **2018**, *11*, 95-117.
- [17]. Bertalosi, V.; Gilli, V.; *Acta Cryst. B* **1982**, *38*, 502-511
- [18]. Bruton, E. A.; Brammer, L.; Pigge, F. C.; Aakeroy, C. B.; Leinen, D. S. *New J. Chem.* **2003**, *27*, 1084-1491.
- [19]. Low, J. N.; Santos, L. M. N. B. F.; Lima, C. F. R. A. C.; Brandao, P.; Gomes, L. R. *Eur. J. Chem.* **2010**, *1*, 61-66.
- [20]. Etter, M. C. *Acc. Chem. Res.* **1990**, *23*, 120-126.
- [21]. Desiraju, G. R. *Angew. Chem. Int. Ed.* **2007**, *46*, 8342-8356.
- [22]. Liu, Y.; Cai, B.; Li, Y.; Song, H.; Huang, R.; Wang, Q. *J. Agr. Food Chem.* **2007**, *55*, 3011-3017.
- [23]. <http://www.chemspider.com/Chemical-Structure.5268628.html>, (Retrieved 01/01/2018)
- [24]. <http://www.chemspider.com/Chemical-Structure.15526334.html>, (Retrieved 01/01/2018)
- [25]. Gilman, H.; Wright, G. F. *J. Am. Chem. Soc.* **1930**, *52*, 2550-2554.
- [26]. CrysAlis PRO 1.171.39.9g; Rigaku Oxford Diffraction, 2015
- [27]. CrysAlis PRO 1.171.39.30d, Rigaku Oxford Diffraction, 2017.
- [28]. McArdle, P.; Gilligan, K.; Cunningham, D.; Dark, R.; Mahon, M. *Cryst. Eng. Comm.* **2004**, *6*, 203-209.
- [29]. Sheldrick, G. M. *Acta Cryst. A* **2008**, *64*, 112-122.
- [30]. Hubschle, C. B.; Sheldrick, G. M.; Dittrich, B. *J. Appl. Cryst.* **2011**, *44*, 1281-1284.
- [31]. Sheldrick, G. M. *Acta Cryst. C* **2015**, *71*, 3-8.
- [32]. Macrae, C. F.; Bruno, I. J.; Chisholm, J. A.; Edgington, P. R.; McCabe, P.; Pidcock, E.; Rodriguez-Monge, L.; Taylor, R.; Van de Streek, J.; Wood, P. A. (MERCURY, CCDC, 2018) *J. Appl. Cryst.* **2008**, *41*, 466-470.
- [33]. Spek, A. L. *Acta Cryst. D* **2009**, *55*, 148-155.
- [34]. McKinnon, J. J.; Spackman, M. A.; Mitchell, A. S. *Acta Cryst. B* **2004**, *60*, 627-668.
- [35]. Wolff, S.; Grimwood, D.; McKinnon, J.; Turner, M.; Jayatilaka, D.; Spackman, M., Crystal Explorer, University of Western Australia Perth, Australia, 2012.
- [36]. Wagner, P.; Officer, D. L.; Kubicki, M. *Acta Cryst. E* **2006**, *62*, o5931-o5932.
- [37]. Zhang, X.; Chen Z.; Li, J.; Lu, T. *J. Chem. Inf. Model.* **2015**, *55*, 2138-2153.
- [38]. Howie, R. A.; Wardell, J. L. *Acta Cryst. C* **1995**, *51*, 2651-2652.



Copyright © 2018 by Authors. This work is published and licensed by Atlanta Publishing House LLC, Atlanta, GA, USA. The full terms of this license are available at <http://www.eurjchem.com/index.php/eurjchem/pages/view/terms> and incorporate the Creative Commons Attribution-Non Commercial (CC BY NC) (International, v4.0) License (<http://creativecommons.org/licenses/by-nc/4.0>). By accessing the work, you hereby accept the Terms. This is an open access article distributed under the terms and conditions of the CC BY NC License, which permits unrestricted non-commercial use, distribution, and reproduction in any medium, provided the original work is properly cited without any further permission from Atlanta Publishing House LLC (European Journal of Chemistry). No use, distribution or reproduction is permitted which does not comply with these terms. Permissions for commercial use of this work beyond the scope of the License (<http://www.eurjchem.com/index.php/eurjchem/pages/view/terms>) are administered by Atlanta Publishing House LLC (European Journal of Chemistry).